Orientation of Borehole and Surface Seismic Stations at Utah FORGE

Patrick Bradshaw[1], Gesa Petersen[1,2], and Kristine Pankow[1]

1 University of Utah, USA,

2 Now at: GFZ Potsdam, Germany,

p.gallagher.bradshaw@gmail.com

ABSTRACT

The Utah Frontier Observatory for Research in Geothermal Energy (FORGE) project is a reservoir-scale field laboratory for testing equipment and techniques necessary for creating Enhanced Geothermal Systems (EGS) with the goal of de-risking the related technologies. The University of Utah Seismograph Stations (UUSS) are responsible for the seismic monitoring of the experiments and have installed a series of permanent surface and borehole seismic instruments around the project site. The horizontal components of these instruments are required to be correctly aligned for seismic source characterization and analysis. Borehole seismometers are installed down a well and the vertical component is the only channel that can be correctly oriented from the time of deployment. Surface station horizontal components can become misaligned through natural phenomena or human error. Here, we further develop the orientation test of the seismic station quality control tool AutoStatsQ, which is based on the polarization of Rayleigh waves on the vertical and radial components. AutoStatsQ returns a preferred correction angle that is the median of the correction angles for all analyzed events. This median value makes uncertainty measurements difficult, while the mean and standard deviation are often biased from single events for

which observed travel paths deviate from simple geometrical assumptions. To address this we build on AutoStatsQ by combining measurements from multiple events with stacking and bootstrapping. This new method is tested on correctly and incorrectly aligned synthetic stations using synthetic waveforms with minor errors. Following the synthetic tests, we use the improved orientation algorithm on stations around Utah FORGE. In the results of this paper, we provide a table with correction angles for all stations of the Utah FORGE network. The surface station correction angles are all within 30° of the correct North and East directions and we recommend adjustments to 2 of the 8 surface stations. The borehole stations could not be oriented during their deployment in the subsurface so correction angles range from -180 to 180 degrees. Besides the methodological improvement, this paper provides correction angles for all stations of Utah FORGE. The systematic survey of the sensor orientations will facilitate and improve future research (e.g., on source mechanisms and shear wave splitting) and therefore help to understand the behavior of the EGS site.

INTRODUCTION

Three component broadband seismometers have become invaluable standard tools for the study and detection of earthquakes. These instruments record seismic velocity in a wide band of frequencies on a vertical channel and two horizontal channels aligned North-South and East-West by convention. During seismic event processing the axes of these stations undergo a rotation transformation to align the horizontal components to be parallel and perpendicular to the direction of wave propagation and are renamed the radial and transverse components, respectively. This is advantageous for analysis for a variety of reasons, including isolating certain wave phases to specific channels (e.g. Ekström and Busby, 2008). SH and Love waves, for example, should theoretically be limited to the transverse component, as the particle motion is horizontal and perpendicular to the direction of wave propagation.

Rotating events is accomplished by using the back azimuth from the station to the event location. This process assumes that the instrument's Z-component is exactly vertical and the orientation of the horizontal components is known. Should the station be misaligned, the transformation to radial and transverse components will also be misaligned and the phase-isolating properties may not manifest. It is thus critically important to ensure that the instrument components are accurately aligned. Surface stations can become misaligned through anything from deployment error to interference from wildlife (Petersen et al., 2019). Borehole seismometers are placed into boreholes or postholes using cable. This installation into vertical holes ensures that the vertical component is correctly aligned, but the horizontal components' orientations are not easily measured. These instrumented wells require alternative methods to determine the true azimuthal orientations of the horizontal component (Ensing and van Wijk, 2018).

These methods include using a controlled source, such as a check shot (Pankow et al., 2020). Alternatively, more theoretical methods such as analysis of the P-wave and Rayleigh-wave polarization (Büyükakpınar et al., 2021; Ekström and Busby, 2008; Petersen et al., 2019; Stachnik et al., 2012; Wang et al., 2016) can be employed. P-waves have particle motion in the direction of wave propagation and at distance will be sensed on the radial component but not transverse, should the horizontal components be correctly rotated into ZRT axes. The particle motion of Rayleigh waves is elliptical in the Z-R plane with a phase shift of 90° observed between the vertical and radial component waveforms.

A major concern holding up more widespread adoption of EGS that Utah FORGE is working to address is the need for a thorough understanding of the induced microseismicity associated with injecting large volumes of fluid into the subsurface. To monitor the well stimulations UUSS, in conjunction with Utah FORGE, has deployed an extensive set of seismic monitoring instruments including eight surface seismometers and seven borehole seismometers. The surface stations were installed by experienced technicians and thus the horizontal components are expected to be accurately oriented with respect to the cardinal directions. Ekstrom et al. (2008) found that most of the USArray Transportable Array (TA) stations in their study were oriented within 0-3° of the correct direction. Some had larger deviations over 10°. In contrast, the downhole instruments are lowered into vertical boreholes using lengths of cables and the only known is that the vertical channel is facing directly down. When the hypocentral distances from the microseismic sources to the instruments are very short it becomes all the more important to have a correct orientation for analyzing wave propagation, structure effects, and inverting for seismic source properties. After introducing the data set and seismic network of Utah FORGE (section DATA), we introduce the orientation test of AutoStatsQ and the further developments (section METH-

ODS). We provide the orientation test results for all surface and borehole stations (section RESULTS) and discuss the observed back azimuthal dependency of the results (section DISCUSSION).

DATA

Seismic Network

The object of analysis in this study are seismic stations installed around the Utah FORGE site (Figure 1). These stations are located on the surface or in shallow boreholes. All are operated by the University of Utah Seismograph Stations and data are available through the EarthScope Consortium (formally known as IRIS). The station names follow a convention that, with the exception of the borehole station FORK, the first 3 letters in any surface station are FOR and the first 3 letters in a borehole station are FSB. The instruments in these stations are themselves largely broadband seismometers. FORK is once again the exception as it does not contain a broadband seismometer but rather a shorter-period OMNI-2400 geophone with a low-corner frequency of 15 Hz and a broadband Silicon Audio accelerometer.

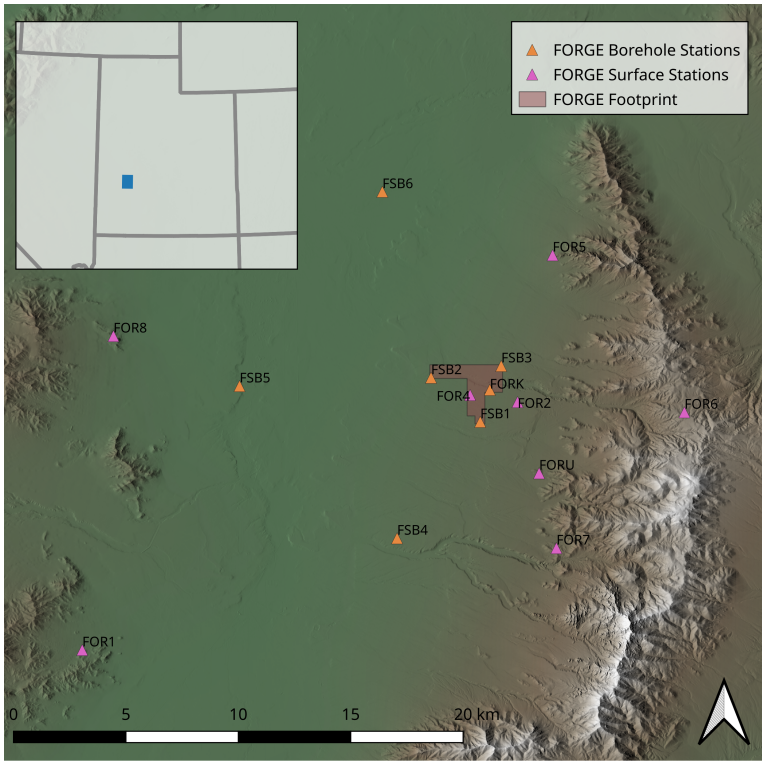

Figure 1: A map of the surface and borehole seismic stations in the Utah FORGE area operated by UUSS. The Utah FORGE site is located in the southwest of the state and abuts the Mineral Mountains to its east. Topography data used is from the USGS Digital Elevation Model catalog (U.S. Geological Survey, 2022).

Teleseismic Catalog

We pull events from the Global Centroid Moment Tensor catalog to build a subcatalog of events that fit specified criteria. The events that are appropriate for analysis are between moment magnitudes of 6.5 and 8, are at least 25 km deep, and have epicentral distances of at least 1000 km. This ensures that the events used in the analytical methods are moderate to deep teleseisms that have magnitudes large enough to be clearly observed while still being reasonably modeled by a point source.

Waveforms

We query the Federation of Digital Seismograph Networks (FDSN) datacenter of IRIS (https://service.iris.edu/fdsnws/) for waveform data from every channel on each station that was recording during a particular teleseismic earthquake. We choose time windows starting 5 minutes before the origin time and include 1.5 hours of data. The long time windows ensure that the full event waveforms are included and that filter effects at the beginning and end of the time windows are minimized.

METHODS

AutoStatsQ (Petersen et al., 2019, https://github.com/gesape/AutoStatsQ) is an application built on the Pyrocko (Heimann et al., 2017, https://pyrocko.org) framework that contains several quality control tests for seismic stations used in source analysis. One of the three tests in AutoStatsQ checks a three component station's horizontal channels for deviation from a North-South and East-West alignment.

The approach to addressing orientation remotely is to use surface waves of well-located teleseismic earthquakes. For a perfectly oriented station that has been rotated to ZRT axes, the Love wave will theoretically be isolated to the transverse component and would not appear on the radial or vertical channels. The Rayleigh wave will appear on the vertical and radial components with a phase shift of 90° between these channels (Stachnik et al., 2012). AutoStatsQ computes a cross-correlation between the radial component and the Hilbert transform of the vertical component at every orientation azimuth. If the rotated components are truly aligned with the direction of wave propagation then the cross-correlation value will be high. If they are not aligned then the Love wave will appear in the radial component and

significantly lower the cross-correlation value. The rotation azimuth that has the greatest cross-correlation value is then compared to the event's previously established back azimuth. This should be done with a significant and diverse set of events that have good azimuthal coverage to account for large-scale crustal structure and path effects.

Figure 2 shows the full process for orienting a station with AutoStatsQ. AutoStatsQ begins this process by querying GCMT for all teleseismic events fitting certain criteria for a given station including date and time ranges, magnitude ranges, depth ranges, and epicentral distance ranges. AutoStatsQ then selects an azimuthally well-distributed subset of these events.

The program downloads miniseed files for every event and saves them locally. The instrument response is removed, a bandpass filter is applied, and the miniseed data is downsampled. Finally, these waveforms are rotated to ZRT axes using the earthquake and station locations. We chose a bandpass with corner frequencies of 0.005, 0.01, 0.2, and 0.22 Hz. We decimate by a factor of 2.

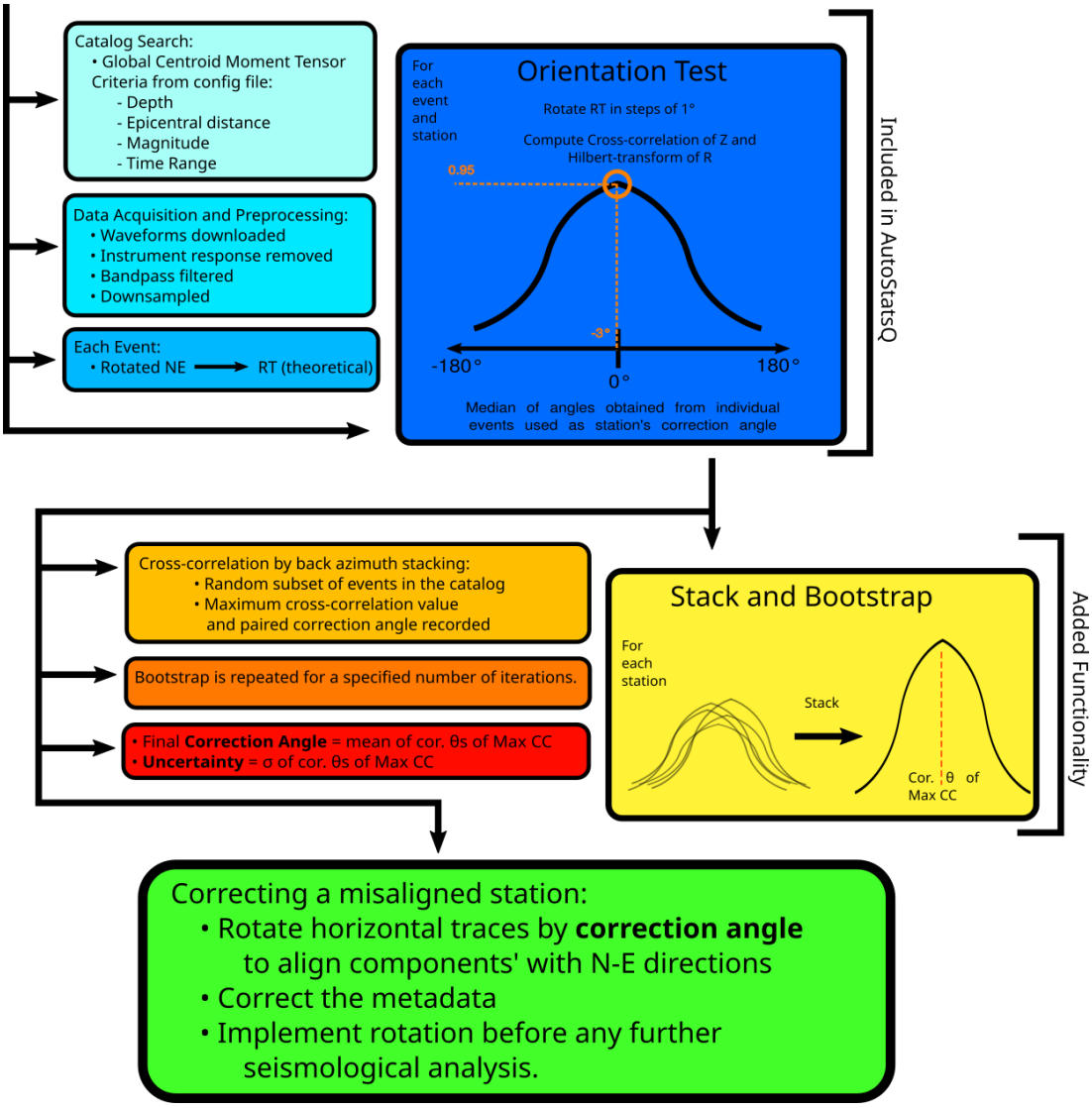

Figure 2: The full orientation test process. It begins by editing the AutoStatsQ configuration file to specify GCMT catalog conditions. The application automatically collects waveforms and processes them for use in the Rayleigh-wave polarization test. For each event in the catalog 360° of cross-correlations are retained. We then initiate a bootstrap where each chain samples from the events and stacks these cross-correlation values. The maximum value from these stacks are collected and the mean is taken as a station correction angle. The blue panels are stages of the orientation test already present in AutoStatsQ and the orange panels are the steps in the new stacking and bootstrapping function.

In order to mitigate back azimuthal dependence on the orientation test process, AutoStatsQ takes a single event from a given azimuthal wedge. We set this wedge width to be a single degree. This gives the orientation process sufficient events to incorporate into the calculations. This is especially important when the station being tested had a limited or recent deployment and thus a smaller pool of valid events. The newest set of borehole stations are FSB4, FSB5, and FSB6 and were deployed in April, 2022. We use 16, 16, and 17 events, respectively. This number of events allows the bootstrapping method to give us meaningful results. We set the minimum cross-correlation threshold for an event to be included to 0.8 to assure good correlation between the vertical component and the Hilbert-transform of the radial component.

The orientation test can be influenced by wave propagation direction if many of the events are arriving from similar back azimuths and thereby pass through the same crustal structure. Blake and Bond (1990) demonstrate that Rayleigh waves are sensitive to surface features and any two teleseismic Rayleigh waves arriving from different back azimuths will have passed through differing structure and undergone unequal scattering. Therefore the median of all event results is the preferred value, rather than the mean. Consequently, if structural influences are present the method lacks a mechanism for adequately quantifying the uncertainty of the orientation direction. Furthermore, some of the events have a poor signal to noise ratio and thus have maximum cross-correlation coefficients that indicate insufficient quality to obtain meaningful results from the orientation test. Once a measurement passes a specified minimum cross-correlation threshold, the results of each event are unweighted so poorer quality arrivals for specific events have the same impact on the result as higher quality arrivals. Setting a low cross-correlation value threshold will thus bias the mean and standard deviation, while a high cross-correlation value threshold will eliminate

events and result in a smaller data set.

To address these issues we developed a new approach in which the cross-correlation values of each correction angle are stacked and normalized. This improves confidence in the correction angle with the maximum cross-correlation value and quickly identifies any problematic patterns like a bimodal distribution or inverted polarities. This method also inherently devalues the input from poorer quality arrivals because the stack of cross-correlation values is less influenced by cross-correlation data with low values.

In order to achieve a robust error estimate without introducing bias through the inclusion of a single event we add a bootstrapping chain to the process. A bootstrap method randomly samples a data set to create data subsets that statistical analysis can be conducted on. For a specified number of iterations we compute the stacked cross-correlation distribution using a randomized subset of the applicable event catalog. Each stack's maximum cross-correlation value and the correction angle at which it occurs is recorded for each bootstrapping chain. This process is illustrated in the second part of Figure 2. If the surface wave orientation method is working correctly then the bootstrapped stacked correction angles should converge around an azimuth with little spread. The standard deviation of the maximum stacked cross-correlation values and orientation angles is an uncertainty measurement that accounts for poor quality arrivals due to the nature of stacking and also can uncover how much influence individual events have on the resulting maximum cross-correlation orientation angle. We found that the bootstrap failed to provide meaningful measurements of uncertainty if the teleseismic earthquake catalog featured fewer than 10 events. We used bootstrap chains of 100 iterations that we found provided a representative spread of maximum cross-correlation values and associated back azimuths should the number of catalog events be 10 or larger. A larger catalog allows more cross-correlations

to be stacked and allows the bootstrap to sample from a larger pool of cross-correlations but this favorable situation requires lengthier deployment times so that enough occasionally occurring teleseismic earthquakes can be recorded.

RESULTS

Testing the Bootstrapping Methodology

We ran the bootstrapped stacking method first on synthetic data that included minor errors. The synthetic stations had cross-correlation coefficient values above 0.95 centered on a correction angle of 0. The stacked cross-correlation by correction angle plot exhibits a unimodal character (Figure 3).

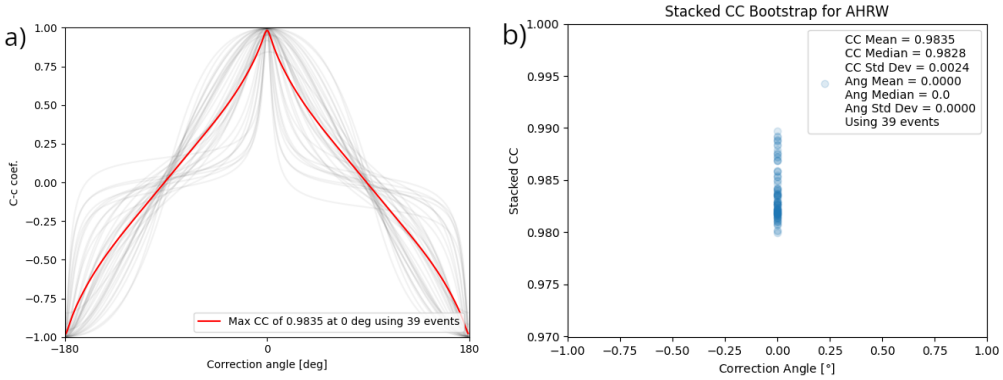

Figure 3: Testing the stacked bootstrapping method on a synthetic dataset. a) a composite of all cross-correlations by correction angle with the stacked value shown in red. A correctly oriented station will have a peak at 0°. The synthetic data has a high cross-correlation maximum at 0.9835 when it is rotated 0° b) After we sample from the cross-correlations and make a stack with the subset (bootstrap) we take the maximum cross-correlation and its paired correction angle and record them for every iteration of the bootstrap. For the synthetic data every correction angle was 0° and had stacked cross-correlation maximum values from 0.98 to 0.99.

As a second synthetic test, we ran the tool on a dataset for which the horizontal components are rotated by 50° after 13 events occur from a total catalog of 38 events (Figure 4). We did this to emulate a temporal change in sensor orientation, which can occur due to human or natural interference. This resulted in bootstrapped maximum cross-correlation values ranging from $\sim$ 0.73 to $\sim$ 0.88. The stacked cross-correlation plot has a visible bimodal character with peaks near 0° and -50°.

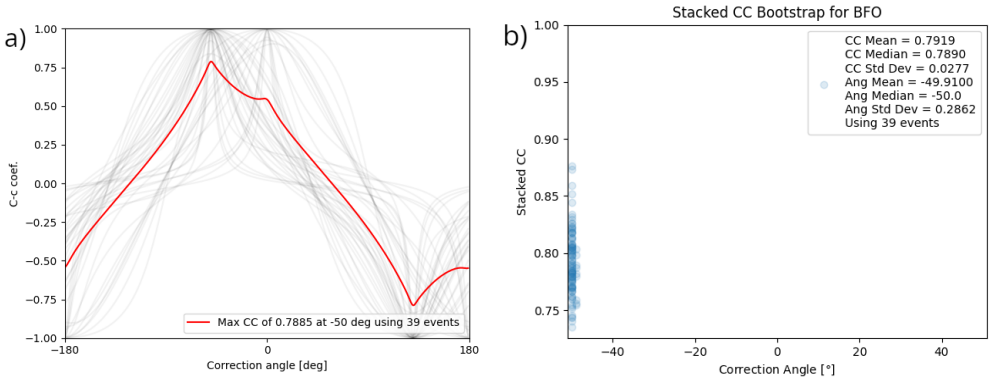

Figure 4: Testing the stacked bootstrapping method on synthetic data for a station that is oriented correctly for 13 events before being rotated 50°. a) The cross-correlation by correction angles shows 2 peaks. One is at 0°, which are from the events occurring before the introduced rotation. The other peak is at -50° and is from events occurring after the rotation. The bimodal character is indicative of a change in orientation. b) The bootstrap for this synthetic test groups tightly around a correction angle of -50° but because some events from before the rotation are sampled the maximum cross-correlation values are lower.

Orientations of Utah FORGE Stations

We apply the bootstrapping cross-correlation method on stations from the University of Utah Seismograph Stations network near the Utah FORGE site. The surface stations are FORU, FOR1, FOR2, FOR4, FOR5, FOR6, FOR7, and FOR8. The borehole stations

were FSB1, FSB2, FSB3, FSB4, FSB5, FSB6 and FORK. As expected, the bootstrapping cross-correlation method indicates that the surface stations are largely oriented correctly. Most have maximum cross-correlation values above 0.9 centered around a correction angle within +/- 10° from a perfect orientation (0°). Six surface stations have correction angles under 10° (Table 1).

Table 1: Correction orientations and standard deviations for FORGE stations. The original AutoStatsQ orientation test returned the median of the correction angle for all events. The Cross-Correlation mean is calculated from the bootstrapped stacks of cross-correlations and the cross-correlation standard deviation is used as the uncertainty. The Angular Mean is calculated from the correction angle derived from the bootstrapped stacks and the uncertainty is the correction angle standard deviation. This Angular Mean is the preferred correction angle from the method. Stations recommended for adjustments and their correction angles are marked in bold and red. Station horizontal components are rotated by the correction angle to align with true North and East directions, e.g., a correction angle of -30° indicates that the station North or SEED channel 1 component points to N30E and therefore needs to be rotated counterclockwise by 30°

Station	**N events**	**Original AutoStatsQ Correction Angle [°]**	**Cross-Correlation Mean $\pm\sigma$**	**Angular Mean $\pm\sigma$[°]**
FOR1	83	0	0.94 ±0.01	-4 ±1
FOR2	48	-1	0.92 ±0.01	-2 ±1
FOR4	14	-6	0.92 ±0.01	-9 ±2
FOR5	25	-24	0.92 ±0.01	**-27** ±1
FOR6	12	3	0.92 ±0.01	0 ±1
FOR7	18	2	0.92 ±0.01	0 ±1
FOR8	18	-15	0.94 ±0.01	**-16** ±1
FORK	23	-103	0.89 ±0.01	**-105** ±1
FORU	35	1	0.91 ±0.01	0 ±1
FSB1	34	104	0.92 ±0.01	**103** ±1
FSB2	38	-118	0.92 ±0.01	**-118** ±1
FSB3	40	-23	0.92 ±0.01	**-24** ±1
FSB4	16	142	0.93 ±0.01	**141** ±2
FSB5	16	-42	0.93 ±0.01	**-45** ±2
FSB6	17	-40	0.92 ±0.01	**-42** ±1

FOR2 is representative of stations that require no adjustments. The cross-correlation by correction angle and bootstap (Figure 5) pull from the cross-correlation by correction angle

results from Figure 6. These show high maximum cross-correlations around 0° correction.

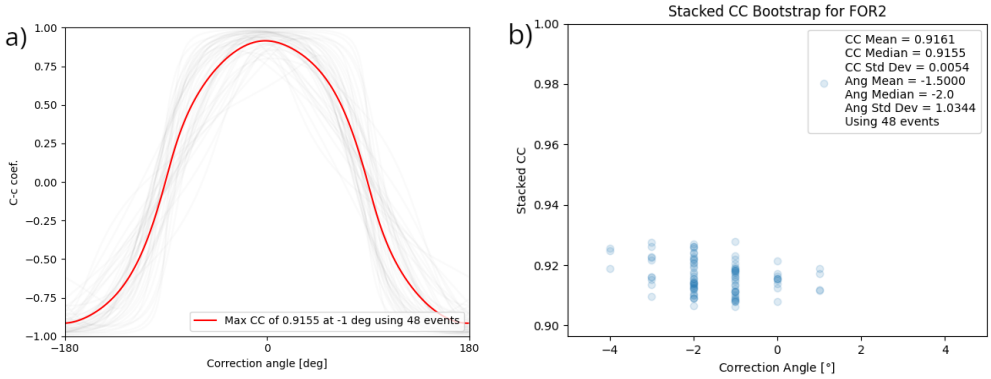

Figure 5: Method results from FOR2 are typical for correctly oriented stations. FOR2 is favored in network operations because of its consistency and it is near the injection site and borehole stations. a) The real station cross-correlation stacks are typically rounder than the synthetic test. The FOR2 stack has a maximum cross-correlation value of 0.9155 at -1°. b) After applying the bootstrapping technique the FOR2 mean returned correction angle is -2°. The small correction angle value leads us to conclude that the station is correctly oriented and does not need adjusting.

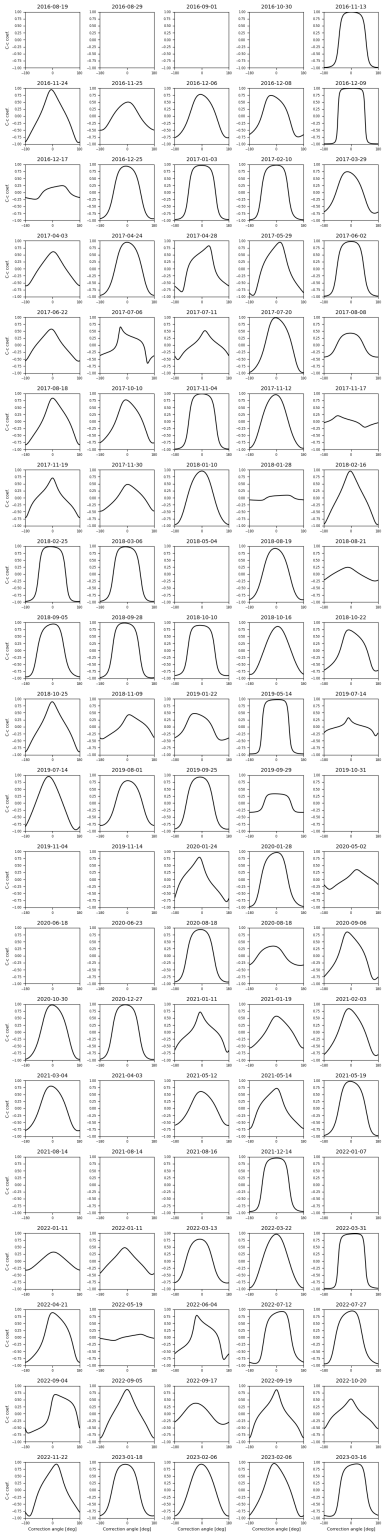

Figure 6: FOR2 has been active for several years and has many events to use in the orientation test.

However, FOR5 is notable as its correction angle is at -27° with a maximum stated cross-correlation coefficient above 0.9 (Table 1). The stacked cross-correlation by correction angle results and the bootstrap results show a tightly-grouped shift (Figure 7). The cross-correlation by correction angle for every used event has a noticeable shift as well (Figure 8).

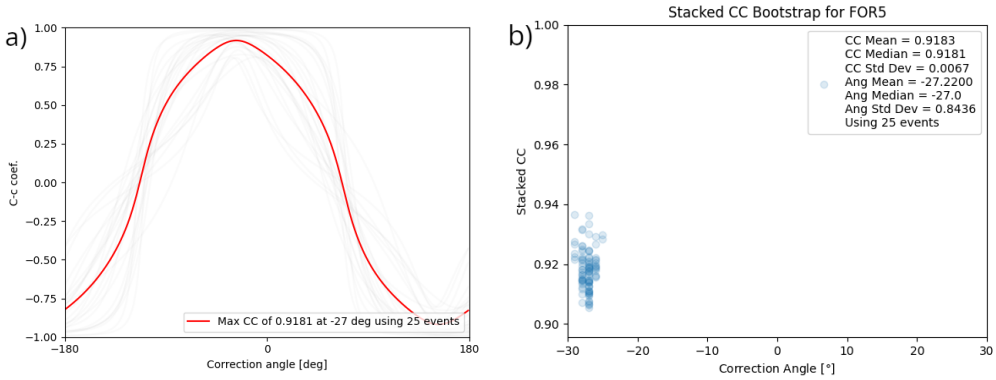

Figure 7: FOR5 is a surface station and was oriented at the onset of its deployment but the orientation method consistently returns a correction angle of -27 degrees. a) FOR5 cross-correlation maximums are shifted off 0°. b) After bootstrapping we have high maximum cross-correlation values of >0.9 that have a mean correction angle of -27° ± 1. FOR5 is therefore misaligned and should be rotated by -27° to have North and East facing horizontal components.

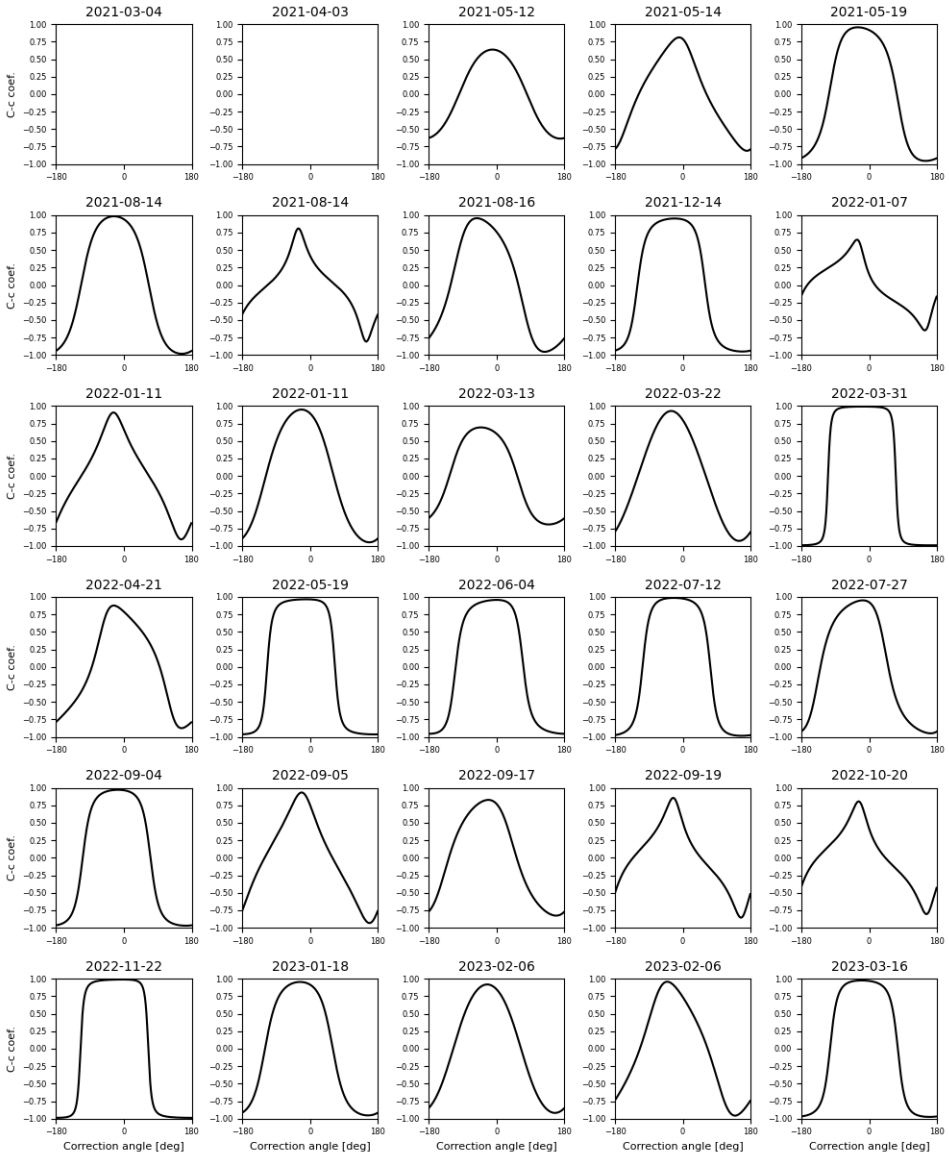

Figure 8: FOR5 is a more recently deployed station and has 25 usable events.

As discussed above, borehole stations FSB1, FSB2, FSB3, FSB4, FSB5, FSB6 and FORK are not oriented so they are expected to have error estimates from bootstrapping similar to the correctly oriented surface stations, but centered on any possible correction angle from -180° to +180°. These stations all have angular standard deviations under 3° (Table 1), which is in agreement with the surface stations distributions (Figure 9).

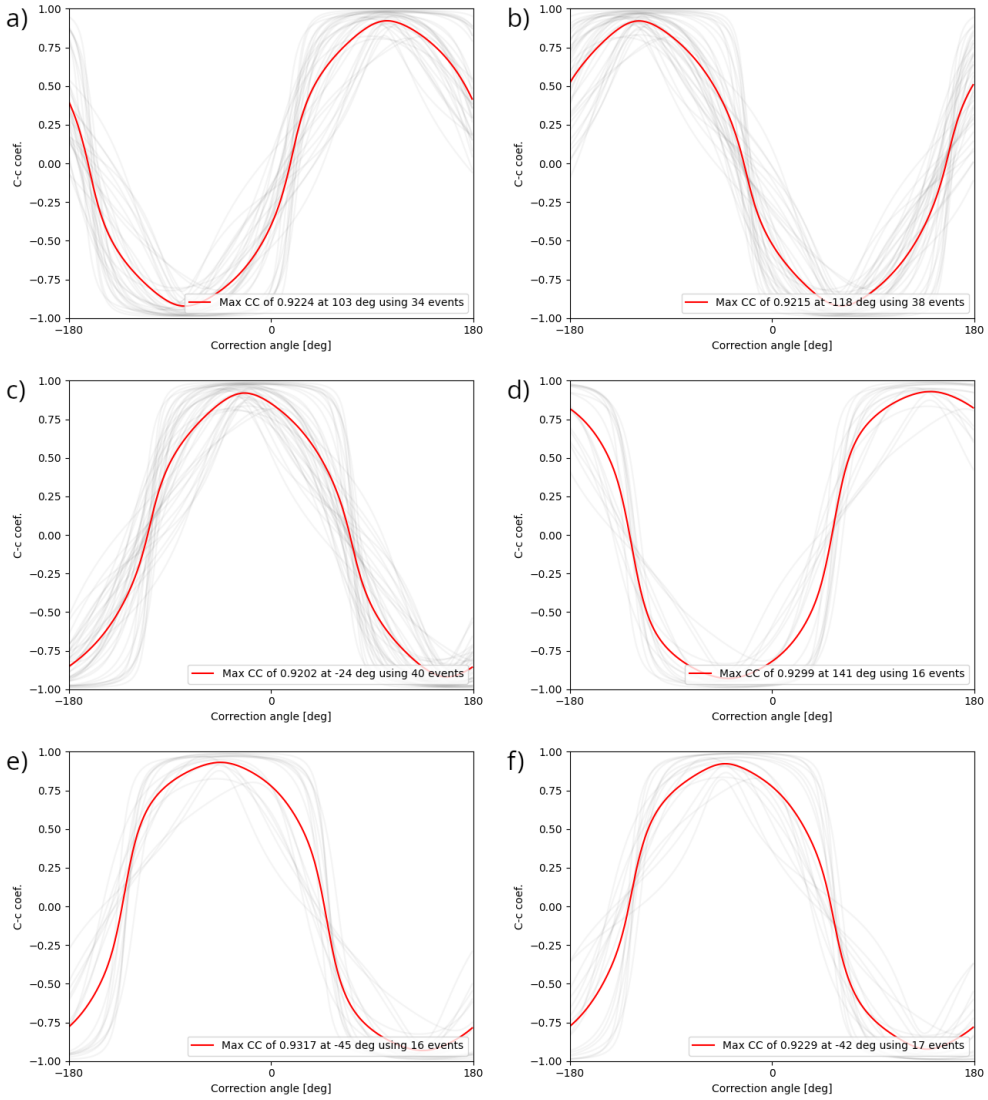

Figure 9: (a) FSB1, (b) FSB2, (c) FSB3, (d) FSB4, (e) FSB5, and (f) FSB6 are all unoriented shallow borehole stations and exhibit a full range of correction angles.

FSB1 is representative of these borehole stations and its correction angle by cross-correlation stack and bootstrap results are shown in Figure 10. The bootstrapped stack of cross-correlation values shows little deviation from 103°. Figure 11 shows every event cross-correlation by correction angle plot that is in the stack or is sampled for use in the bootstrap. Most events have maximum cross-correlation values of about 0.8.

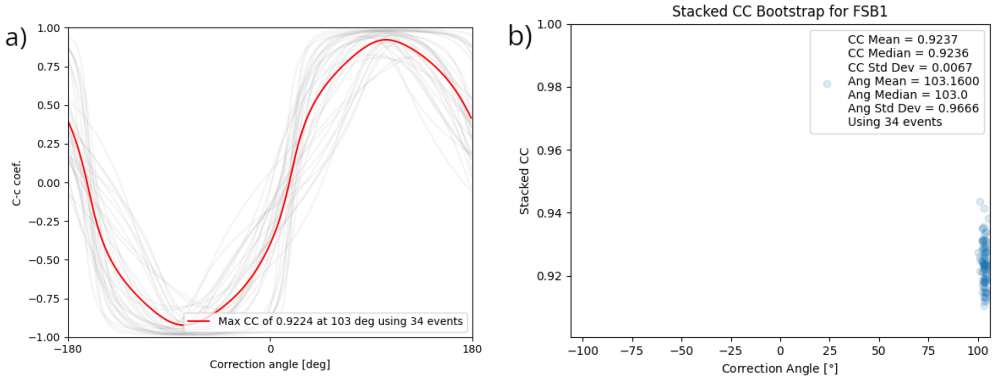

Figure 10: FSB1 is a shallow borehole station and was not oriented during deployment. The orientation method returns a consistent correction angle of 103 degrees. a) The stack shares the same shape with the FOR2 and FOR5 stacks (Figures 5 and 7). Its large correction angle is reasonable due to the circumstances surrounding its deployment. b) The bootstrapped maximum cross-correlation by correction angle values are tightly grouped with high cross-correlation values >0.9.

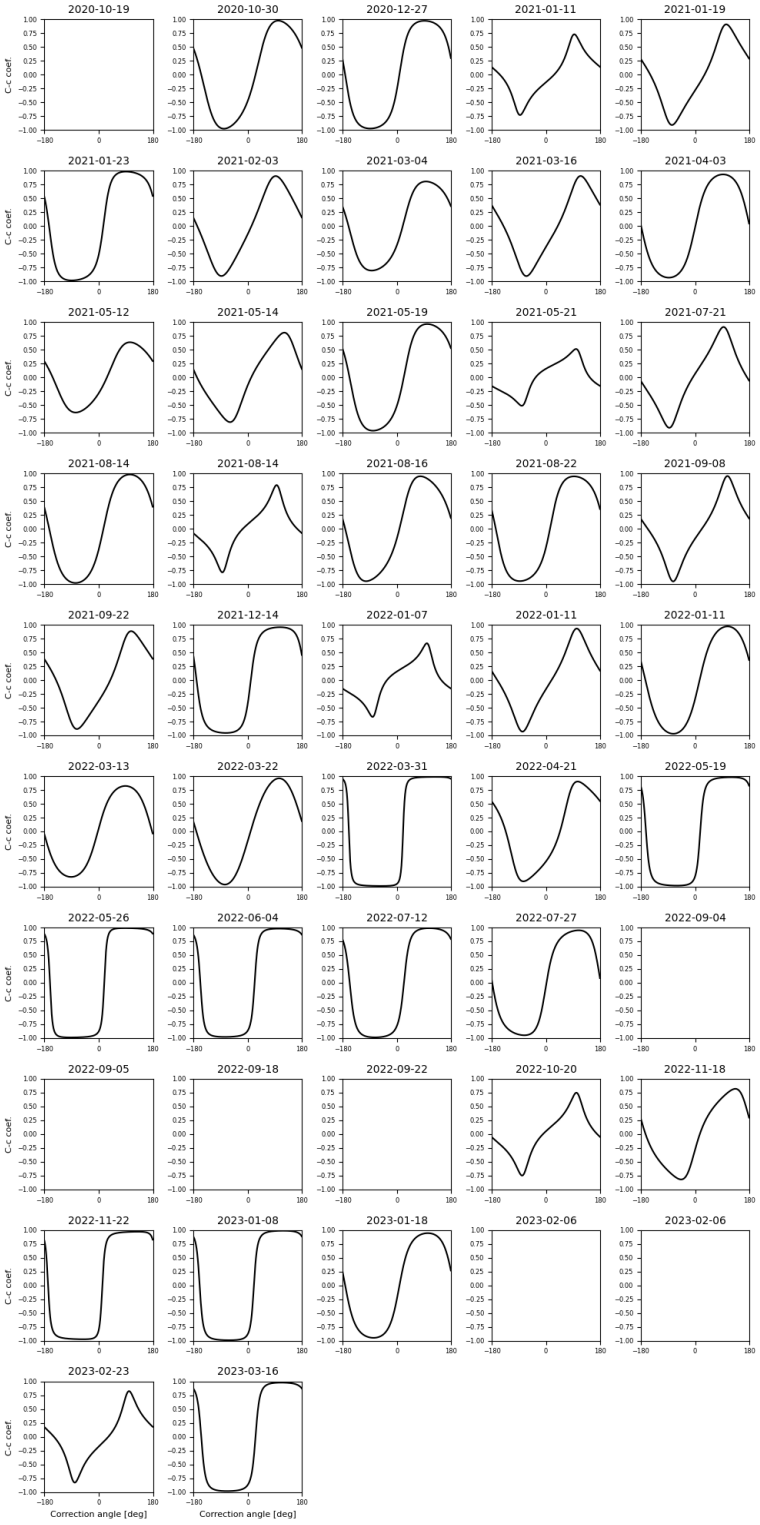

Figure 11: FSB1 has been deployed long enough to use 34 events.

FORK - Additional Orientation and Polarity Checks

The FORK station required several additional tests to ensure that the calculated correction angle was valid. FORK is equipped with a strong motion Silicon Audio accelerometer and a short period OMNI-2400 sensor. The short period sensor has a low-frequency corner of 15 Hz (Geospace Technologies Corporation) making it inappropriate for use with AutoStatsQ's teleseismic surface wave operations, which typically have frequency content of $<<$ 0.1 Hz. Instead we used the colocated accelerometer that is rated as having a passband of 0.004 to 800 Hz (Silicon Audio Seismic). AutoStatsQ's restitution methods properly integrate both velocity and acceleration sensors to displacement.

Before conducting the orientation tests on FORK we needed reassurance that the vertical component was properly wired and that its polarity was correct. First, we searched through the USGS catalog for a large, deep, teleseismic earthquake that occurred during a time when both FORK and FOR2 were online and recording. We used FOR2 as a benchmark not only because it is geographically close but also because it is a reliable station in the area when used in network monitoring operations. A M_W 7.6 magnitude earthquake occurred in southern Mexico at 18:05:08 on September 19th, 2022, at a depth of 26.9 km. This event fulfilled the quality requirements for being used for tests. We used the Pyrocko Python library to remove the instrument response and integrated to displacement waveforms. Because of the nearly identical travel paths the signal at both FORK and FOR2 should be similar. Figure 12 shows that FORK and FOR2 have similar traces and therefore have parallel vertical components.

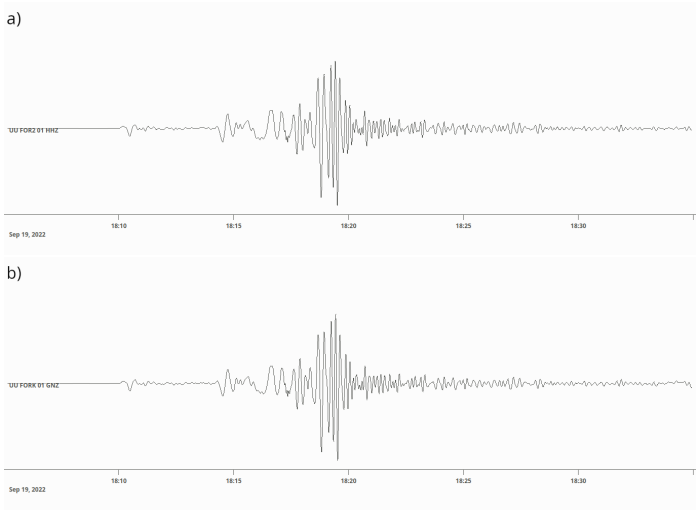

Figure 12: The M_W 7.6 Mexico earthquake occurring on Sept. 19, 2022, at 18:05:08 on (a) FOR2 and (b) FORK. The instrument response was removed using Pyrocko. The signal is similar across both traces.

With confidence that FORK's vertical component is correctly oriented we next needed to ensure that the station was following the right-hand rule convention. For a broadband surface station that has a downward facing vertical channel this typically entails a North and East channel. This could be ordered as [HHN, HHE, HHZ] in cases where the right-hand rule must be maintained. As discussed earlier, FORK is a borehole station and instead of a North, East, and vertical channel it has a "1", "2", and vertical channel for both the accelerometer and short period sensor. The relative positions of the GN1 and GN2 components are necessary information that must be determined before AutoStatsQ can be used to orient the station. Should the station be miswired or perhaps not follow a right-hand rule convention then the correction angle could be off by 90° leading to the transverse and radial components being perpendicular to their correct axes, effectively swapping. A simple check is to rotate the GN1 channel by 90° and see if it is identical to or inverse from the GN2 channel. We see in Figure 13 that the traces are identical and thus the station

does follow the right-hand rule.

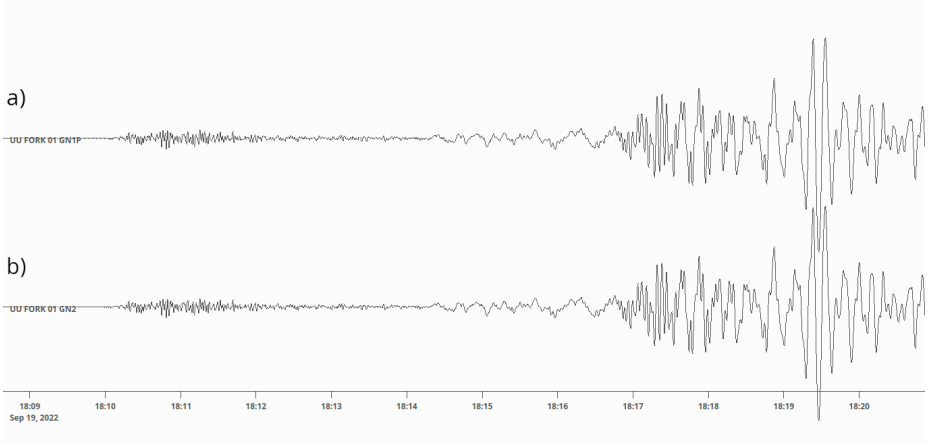

Figure 13: Channel (a) GN1 was rotated by 90° and saved as GN1P and compared to an unrotated (b) GN2. The traces are identical, demonstrating that [GN1, GN2, GNZ] follows the right-hand rule.

We did a final test using the southern Mexico event in conjunction with the returned correction angle from AutoStatsQ. Figure 14 illustrates the process of starting with an AutoStatsQ determined correction angle and arriving at ZRT axes. Using the AutoStatsQ rotation angle for FORK of -105°, we rotate the station GN1 component to the back azimuth of the Mexico event. We then examined the traces to determine if any of the phase isolating properties of the ZRT rotation were observable. Figure 15 shows the P-wave arrival at FORK with a noticeably larger amplitude on the radial and vertical components, which is expected as P-wave's particle motion is parallel to the direction of wave propagation. The surface wave arrivals also show similarity between the radial and vertical components in terms of envelope shape and pre-arrival signal. The wave packet arriving between 18:17 and 18:18 is of noticeably larger amplitude on the transverse component, which could indicate a Love wave arrival. The characteristics of the body and surface waves are in line with what is theoretically expected should FORK be correctly oriented.

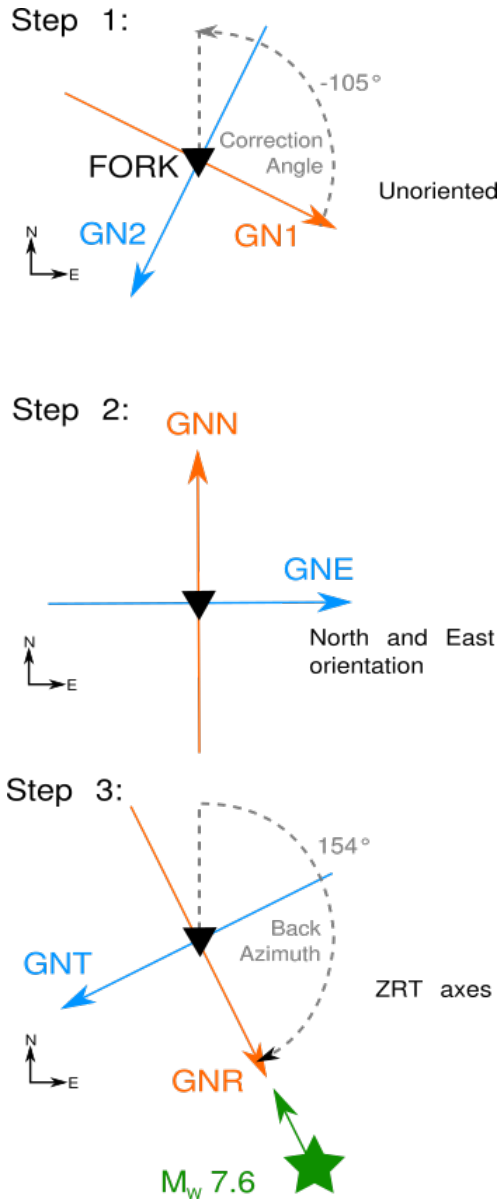

Figure 14: Rotating to ZRT from an unoriented borehole station. Step 1: Station horizontal components are not aligned North and East. The AutoStatsQ orientation test returns a correction angle of -105°. Step 2: After rotating the horizontal components -105° they are correctly facing North and East. Step 3: The back azimuth to the event source is 154° so rotating the North and East components by this angle will result in ZRT axes.

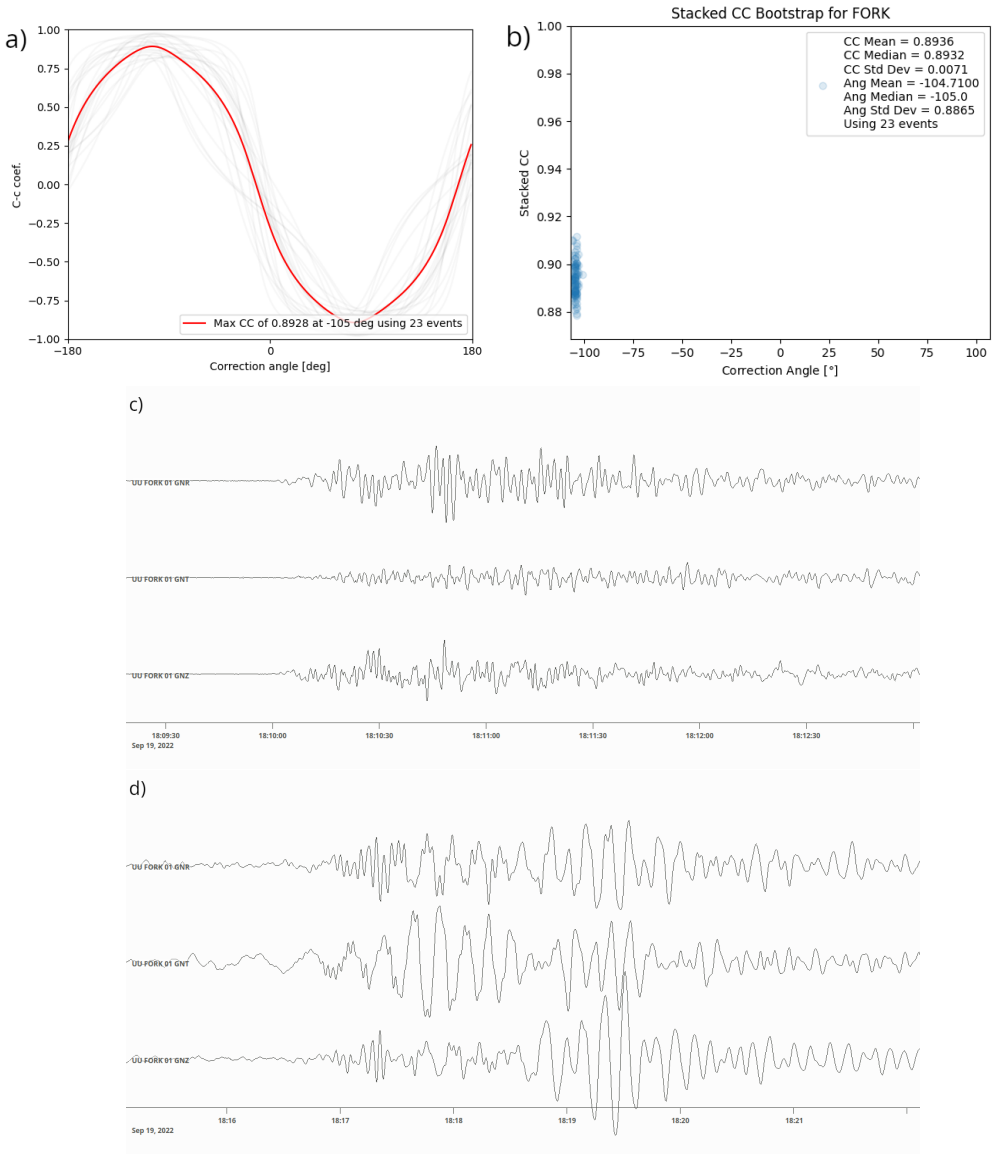

Figure 15: After (a) stacking and (b) running the bootstrapping procedure, AutoStatsQ returns a correction angle for FORK of -105°. c) After correcting and then also rotating to ZRT using the back azimuth to the southern Mexico earthquake, we can see that the P-wave arrival is strongest on the radial and vertical components and weakest on the transverse component. d) When looking at surface waves we can see that the radial and vertical have a closer resemblance and that there is an earlier arrival on the transverse component absent on the others, indicative of a Love wave arrival.

DISCUSSION

One potential contributor to variations in back azimuth are teleseismic path differences. Figure 16 shows the sensor orientation correction as a function of teleseismic back azimuth for stations FOR1 and FOR2.

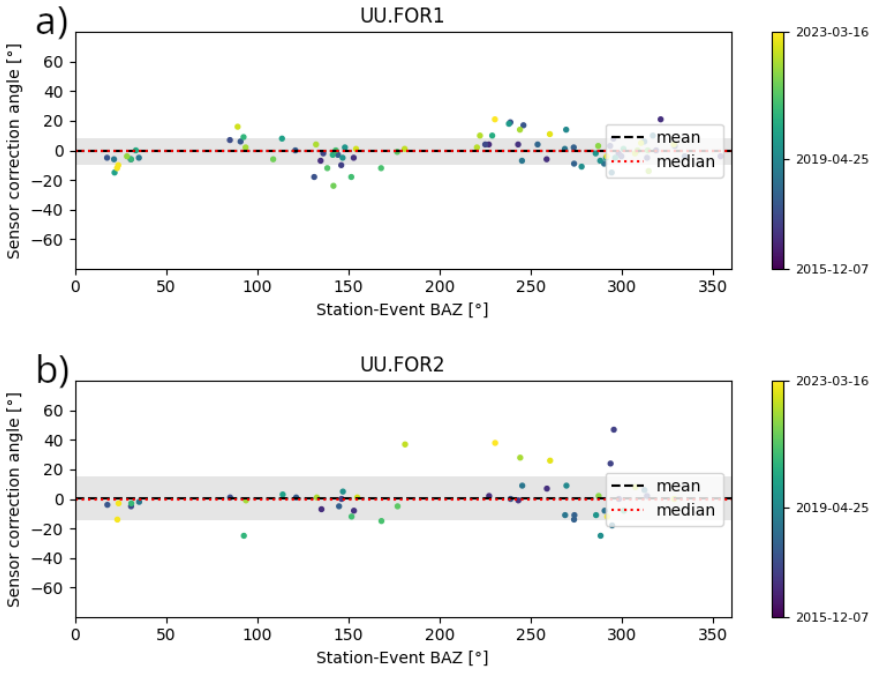

Figure 16: The back azimuth for each event and the calculated maximum cross-correlation angle for stations (a) FOR1 and (b) FOR2. The mean, median, and standard deviation are from the original AutoStatsQ orientation test without stacking.

The station corrections for FOR1 appear to be grouped by event back azimuth. There is a small cluster of 9 events with negative correction angles ranging from -4° to -18° centered around the back azimuth of 20°. Another grouping of positive correction angles ranging from 2° to 21° is centered around a back azimuth of 240°. Starting at a back azimuth of 80° the correction angles begin at positive values of $\sim$ 10° and appear to trend negatively ending at a back azimuth of 170° with a negative correction angle $\sim$ -15°.

Another station with a significant number of events is FOR2 (Figure 16). We can see that most events are close to 0° but the events with relatively larger correction angles are somewhat grouped around back azimuths of 180° and 300°. The groupings with low correction angles share relatively similar directions with FOR1.

The grouping around a back azimuth of 20° is also present with near single-digit negative correction angles. The range of back azimuths from 80 to 170° has events with positive correction angles at the lower back azimuths and trends negative as the back azimuth increases. The grouping around a back azimuth of 240° has events with near 0° correction angles but has 2 events of 13° and 22°.

FOR1 and FOR2 use some of the same events that return similarly anomalous correction angles. The magnitude 8.1 earthquake occurring on 3/4/2021 at 19:29 near Kermadec Islands, New Zealand, has a back azimuth from FOR1 and FOR2 of 232° and has a correction angle of 11° and 22°, respectively. The Kermadec Islands, just north of New Zealand are due southwest from Utah. FOR1 and FOR2 also share the 23:37 1/23/2021 magnitude 7.0 earthquake near South Shetland Islands, the 5:23 2/3/2021 magnitude 6.6 earthquake near West Chile Rise, and the 18:35 8/12/2021 magnitude 8.3 earthquake near the South Sandwich Islands. These events are at a back azimuth of 155°, 168°, and 143° respectively and have correction angles all ranging from -12° to -18°. These events are sourced in or around the southern end of South America and due south-southeast.

FOR1 and FOR2 have preferred correction angles of -4° and -2° respectively. Both of these stations share relative similarities in their correction angle by event back azimuth relationships. This indicates that the incoming teleseismic surface waves are being influenced by structure and are resulting in a difference in correction angles ranging from $\sim$ +/- 20°

at maximum. This seeming back azimuthal dependence on correction angle is problematic but the stacked bootstrap method resists these influences on the preferred correction angle. Determining which crustal structures are influencing the results is beyond the scope of this study but their presence itself is noteworthy and a potential topic of further investigation. A further development of the method could incorporate relative station orientation deviations in relation to other nearby stations in the network.

The AutoStatsQ orientation test has some dependence on back azimuth but is still able to give us confidence in the orientations of the horizontal components of the Utah FORGE seismic stations operated by UUSS. We are able to identify slightly misaligned surface stations and able to determine orientations for unoriented borehole stations. The bootstrapping method returns correction angles that are close to the median correction angle that AutoStatsQ previously returned as its preferred correction angle but we have a more robust estimation of error in the bootstrapped angular mean and standard deviation.

CONCLUSIONS

In this study we further developed the station orientation test included in AutoStatsQ by stacking cross-correlation values and implementing a bootstrap that returns correction angles with more meaningful measurements of uncertainty. We tested the method on synthetic data and determined it was capable of detecting misaligned stations and returning their correction angles. We then used the method to analyze the Utah FORGE network and validated six surface station orientations, determine correction angles for two identified misaligned surface stations, and provide orientations for seven previously unoriented borehole stations. This method can be used in future studies as a quality control test for surface stations or as a orientation process for unoriented borehole stations. We discuss the back

azimuthal dependency of the returned correction angles and the implications of the method sensitivity to crustal structure but through detailed analysis find stable results.

ACKNOWLEDGMENTS

Funding was provided by DOE EERE Geothermal Technologies Office under Project 429 DE-EE0007080 Enhanced Geothermal System Concept Testing and Development at the Milford City, Utah Frontier Observatory for Research in Geothermal Energy (FORGE) site and the State of Utah. Waveforms from FORGE stations are available through the University of Utah Seismograph Stations (https://quake.utah.edu/FORGE-map) and through Incorporated Research Institutions for Seismology (www.iris.edu/hq/; network code UU)

REFERENCES

Blake, R. J., and L. J. Bond, 1990, A general model for rayleigh wave — surface feature scattering problems.

Büyükakpınar, P., M. Aktar, G. Maria Petersen, and A. Köseoğlu, 2021, Orientations of Broadband Stations of the KOERI Seismic Network (Turkey) from Two Independent Methods: P- and Rayleigh-Wave Polarization: Seismological Research Letters, **92**, 1512–1521.

Ekström, G., and R. W. Busby, 2008, Measurements of Seismometer Orientation at USArray Transportable Array and Backbone Stations: Seismological Research Letters, **79**, 554–561.

Ensing, J. X., and K. van Wijk, 2018, Estimating the Orientation of Borehole Seismometers from Ambient Seismic Noise: Bulletin of the Seismological Society of America, **109**, 424–432.

Geospace Technologies Corporation, n.d., OMNI 2400 high-temperature geophone: Specifications brochure.

Heimann, S., M. Kriegerowski, M. Isken, S. Cesca, S. Daout, F. Grigoli, C. Juretzek, T. Megies, N. Nooshiri, A. Steinberg, et al., 2017, Pyrocko-an open-source seismology toolbox and library.

Pankow, K., M. Mesimeri, J. McLennan, P. Wannamaker, and J. Moore, 2020, Seismic monitoring at the utah frontier observatory for research in geothermal energy: Proceedings of the 45th Workshop on Geothermal Reservoir Engineering, Stanford, CA, USA, Nature Publishing Group, 10–12.

Petersen, G. M., S. Cesca, M. Kriegerowski, and the AlpArray Working Group, 2019, Automated Quality Control for Large Seismic Networks: Implementation and Application

to the AlpArray Seismic Network: Seismological Research Letters, **90**, 1177–1190.

Silicon Audio Seismic, n.d., Silicon audio model 203 low noise accelerometer: Specifications sheet.

Stachnik, J. C., A. F. Sheehan, D. W. Zietlow, Z. Yang, J. Collins, and A. Ferris, 2012, Determination of New Zealand Ocean Bottom Seismometer Orientation via Rayleigh-Wave Polarization: Seismological Research Letters, **83**, 704–713.

U.S. Geological Survey, 2022, USGS 1/3 arc second n39w113 20220510.

Wang, X., Q. Chen, J. Li, and S. Wei, 2016, Seismic Sensor Misorientation Measurement Using P-Wave Particle Motion: An Application to the NECsaids Array: Seismological Research Letters, **87**, 901–911.